International Journal of Engineering Research and Technology. ISSN 0974-3154, Volume 14, Number 1 (2021), pp. 22-40

Structural Analysis of Thin Films on basis of MATLAB by LIBS

Omaro A. Azouz[1] and **Kemal Efe Eseller**[2]

[1]*Electrical and Electronics Engineering Department, Engineering College/ Atilim University, Turkey.*

[2]*Electrical and Electronics Engineering Department, Engineering College/ Atilim University, Turkey.*

ORCIDs: 0000-0002-9758-4852 (Kemal Efe Eseller), 0000-0002-7919-0366(Omaro Azouz)

Abstract

Laser induced breakdown Spectroscopy (LIBS) is a type of atomic emission technique that used the laser shot on specific area of the sample to atomization-cum-excitation process , which released photon (light) at different wavelengths ,which can be after that used to determine elements in each sample and its concentration, in our work we develop a MATLAB code to determine the peaks and they are under the peaks with using Lorentzian fitting, so that we can calculate the Area percentage under each peaks and we compare the results with other two ways by using Origin software and Excel , so that we have the ability to calculate the RSD ,LOD and SNR and the noise Fluctuation for each shot that we had at every wavelength, the sample was prepared and we used the LIBS Type ((LPS-1064-A 50mJ) , Start Wavelength 186.263 nm, End Wavelength: 888.604 nm, Gate Delay: 0.350 ,Gate Width (ms) :1.050 , Laser Output Level :0.000 ,X Position: 0.000 ,Y Position: 0.000 ,Z Position: 0.000 , the calculation by using certain program showed identic results regards the Area -percentage under each peaks just we see a very abnormal response on the first and second shot at each wavelength after that the photon emission effect goes ordinary . our collected intensity data have been compared with the NIST data. The sample was continued: SN, Mg, Fe, Al, Cu, S, Si, Zn.

Keywords: LIBS; Lorentzian fitting; software, thin films, MATLAB

I. INTRODUCTION

Each atom has unique emission characteristic, which called the photoelectric effect , that refers to the emission, or ejection, of electrons from the surface of, generally , a metal in response to incident light (photon), where we can use this information (Intensity of light) to analyses the composition of any sample , by using the classical Maxwell wave theory of light, the more intense the incident light the greater the energy with which the electrons should be ejected from the metal [3]. That is, the average energy carried by an ejected (photoelectric) electron should increase with the intensity of the incident light. Laser induced breakdown spectroscopy(LIBS) is an emission analysis tool that used for very quick analysis without need to preparation of a sample ,regardless to its state (Gas-liquid-solid) ,and it caused no damage at the sample ,because the investigated area is very small and the time for laser shots is very short . Excited sample is taken to a gaseous plasma state and dissociated to all molecules and fine particles, which produces a characteristic plasma light. Intensity of this plasma light is associated with concentration of the elements in the sample [1],[2],[3],[4].

We used LIBS Type (LPS-1064-A 50mJ) , Start Wavelength 186.263 nm, End Wavelength: 888.604,Gate Delay: 0.650 ,Gate Width (ms) :1.050 , Laser Output Level :0.000 ,X Position: 0.000 ,Y Position: 0.000 ,Z Position: 0.000 , 13 mJ, for the investigation process with ten shots at each step of wavelength. The laser that focused on the sample created a plasma , one of the characters of the LIBS ,that deals with a low-energy pulsed laser (typically tens to hundreds of milli joules per pulse) to generate a plasma which vaporizes a small amount of the sample[5]. Spectra emitted by the excited species, mostly atoms, are used to develop quantitative and qualitative analytical information. which it begins , when the atoms are excited , to start to move to upper orbit-level and rapid forward back to ground level and at this time the photon are released with unique wavelength[6] [7], these intensities of the photon (light) can be collected and analyzed to determine the elements of the sample and percentage of each elements in it. In our study case we wrote a MATLAB-code to determine the peaks and their area under each of them, we used Lorentzian fitting procedure to obtain the curve fitting to have a good result [6]. Our sample was a thin film sample , that was produced by using the chemical vapor deposition (CVD) , this process has many advantages such as versatile, obtained high purity and density and the metal formation is underneath the melting point [7]., Through the collected data we calculated the SNR for each peak at each shot,, Noise fluctuation for each peak at each shot , determine RMS ,RSD, Area percentage and SNR at each wavelength , the collected data from our LIBS is processed additionally by Origin, Excel and as well as the written MATLAB code so that we can compare the results with each other, in order to optimize the MATLAB code, and to be ready to be used in practice very efficiently.

Due to the LIBS workwise, shot to shot error will differ from each other. Main result of this error is the background noise in the spectrum of the plasma created. LIBS is rapid investigating technique. On the other hand, this quick and easy way of data measurement brings errors in every single spectrum of data taken from the sample and every error would be different from the other. The plasma in our experiments is created in the air, it is obvious that in every single plasma created, there will be other accompanying species in different concentrations in the air just in front of the sample. and as the laser beam is ablating the sample surface in every single shot, the shape of the target surface area is changing. Due to this change, laser energy absorbed by the sample is changing shot by shot as well. To avoid the error coming from every shot, SNR is calculated with peaching on the noise fluctuation with the max. of the signal .

International Journal of Engineering Research and Technology. ISSN 0974-3154, Volume 14, Number 1 (2021), pp. 22-40

II. THIN FILM SAMPLE'S PREPARATION

Our sample was prepared through Chemical Vapor Decomposition (CVD), which it was used to secure high purity and density in our sample[10], the metal formation through this process is below the melting point. The thick of our sample was approximately 12 µm.

III. LIBS EXPERIMENTAL SETUP

For recording the data we used LIBS Type (LPS-A-1064 50 200 mJ) , with Start Wavelength 200 nm, End Wavelength: 462, Gate Delay: 0.350 ,Gate Width (ms) :1.050, Laser Output Level :0.000 ,X Position: 0.000,Y Position: 0.000 ,Z Position: 0.000, the lenses that have been used was convex lens (N-Bk7-Bi)[9], for the directed laser pulse on the sample and for spectrum lights ,such as the one ,that directed to the fiber optics acceptance cone, the collected LIBS spectra data is collected by Thorlabs CCD-spectrometer. LIBS system used to consist of: Power Supply, Control screen, Laser Head, Cooling Unit, Target holder, to stabilize the samples and to move them gradually with a compass, the light collection system (lens, fiber optic) that is collecting the light created by the spark and transports the light to the detection system, the system schematic is shown in Figure 1, [2].

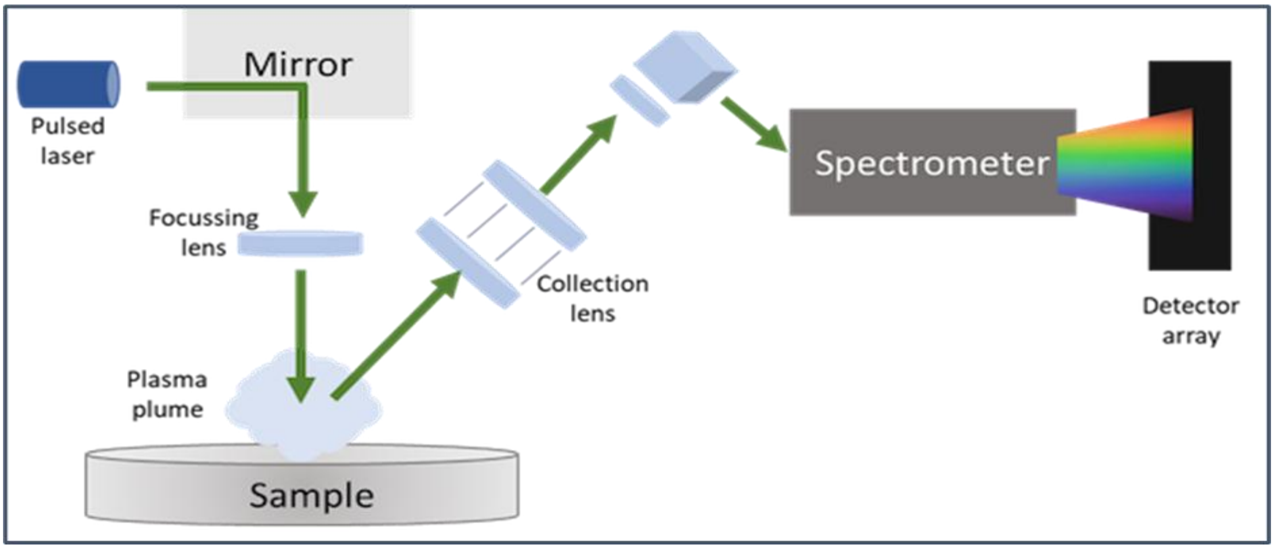

Fig 1. Schematic for LIBS system

The collected data from the LIBS system are represented in fig 2-a and fig 2-b

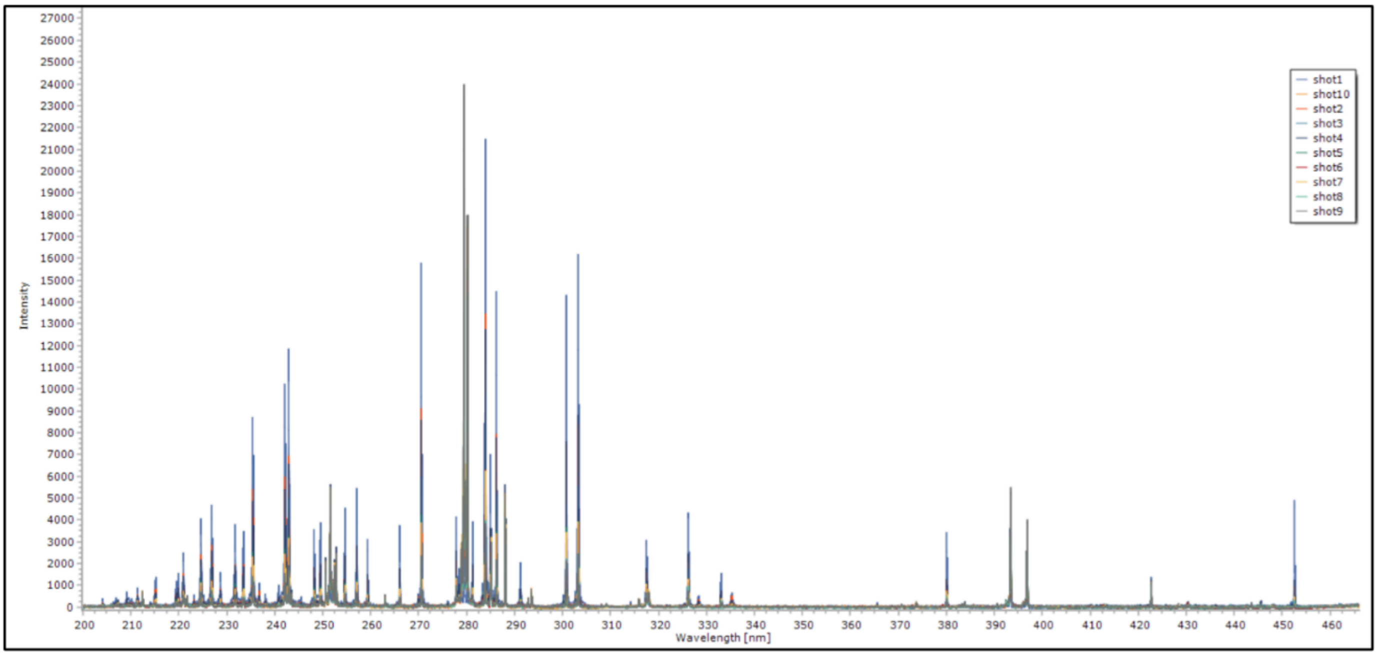

Fig 3(a). 10 shots Intensities)

International Journal of Engineering Research and Technology. ISSN 0974-3154, Volume 14, Number 1 (2021), pp. 22-40

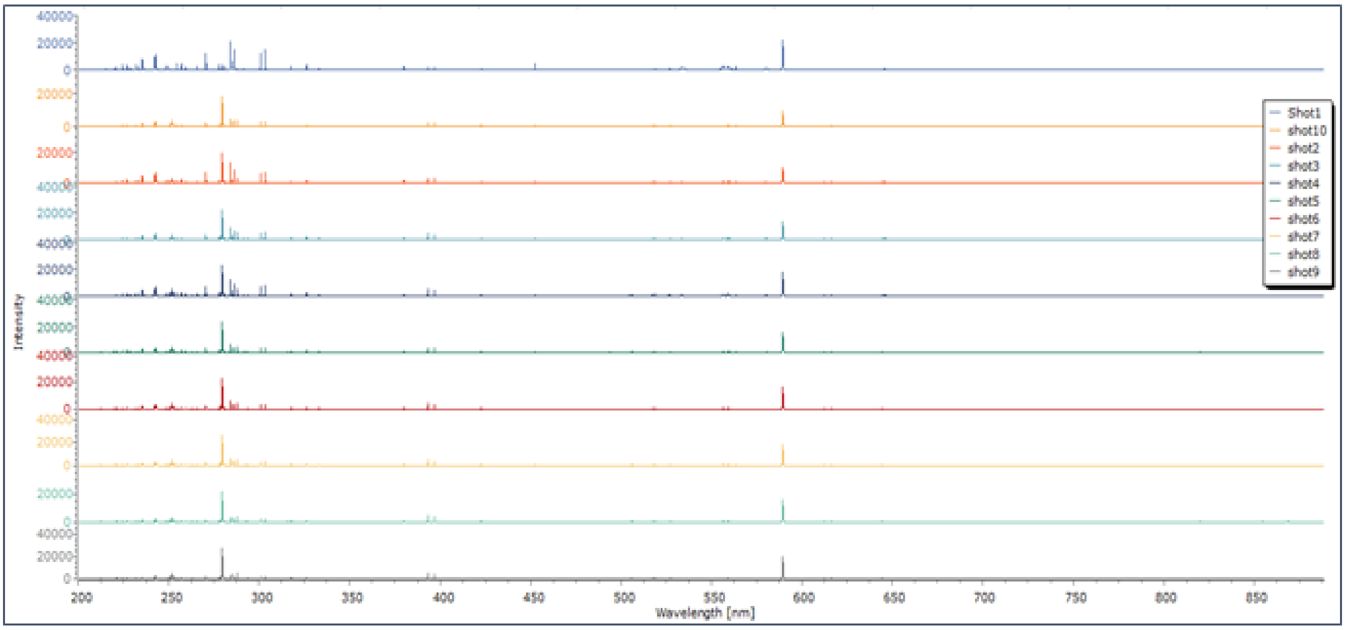

Fig 2(b). 10 shots Intensities stack spectra

IV. DATA ANALYSIS

V.I prepared of Data

Our data after finishing the experiment was in 77 table with 10 shot for every table, firstly we calculated the average of all the tables so that we have one table, which includes 10 shots, the average was calculated by the formula [8]

$$\bar{x} = \sum_{i=1}^{n} \frac{x_i}{n} \qquad \text{[equation 1]}$$

where,

$\bar{X}$ is the average value of the Intensity

Σ Xi is sum of Intensity value at each shot

which was gave us an end table, that showed like in Table 1 below

Table 1. 10 shot end table

Wavelength [nm]	shot1	shot2	shot3	shot4	shot5	shot6	shot7	shot8	shot9	shot10

IV.II Data Analysis

i. RSD (Relative Standard Deviation)

Relative standard deviation is calculated to understand the error of the system itself. This error is appeared, because the surface of the sample is distributed so that the focal spot of the laser is not same for each consecutive laser pulse and due to changing media conditions (varying particles in front of the sample) in every shot, the absorbed partition of the laser beam is changing accordingly. shot by shot both factors cause fluctuations and poor reproducibility of the LIBS data. We calculated the for each wavelength, the relative standard (RSD) shows us clearly, whether the normal standard deviation is a smaller or larger amount compare deviation to the statistical average of the data set, that we collected from the practical experience[7].

$$RSD(\%) = \frac{100}{N_{conc}} \sum_{k=1}^{N_{conc}} \frac{\sigma_{C_k}}{C_k}$$

with $$\sigma_{Ck}{}^2 = \sum_{i=1}^{\rho} \frac{(\hat{c}_{ik}-c_k)^2}{\rho-1} \qquad \text{[equation 2]}$$

where,

N_{conc}= number of different concentrations in the validation set

ρ=number of spectra per concentration

σ=Standard deviation

ii. RMS (Root mean square)

The collected data was positive and negative so that, we choice to determine the Root mean square (RMS) [2], through it we can measure the dispersed of the quantity around the average value in other words, the average value through (RMS) is not removed as when we used the standard deviation (STDEV), and through this rms we can define the size of signal (strength of the signal) we used the formula

$$\mathbf{RMS} = \sqrt{\frac{\sum_{i=1}^{N} x_i}{N}} \qquad \text{[equation 3]}$$

Where,

Σ Xi is sum of Intensity value at each shot

N is the length of the system at every shot

International Journal of Engineering Research and Technology. ISSN 0974-3154, Volume 14, Number 1 (2021), pp. 22-40

iii. SNR(signal Noise Ratio)

The signal to noise ratio (SNR) is very important to determine the strong of the signal at certain wavelength, which carried information, we calculated the SNR for every wavelength between the 10 shot [2],[12].

$$SNR= {\textbf{Signal power}}/{\textbf{Noise Power}} \qquad \text{[equation 4]}$$

where,

Signal Powe is the average at every certain wavelength for the 10 shots

Noise Power is the Standard deviation at certain wavelength for the 10 shot

SNR = STD Baseline Fluctuation / Max. Intensity for every spectrum line observed [equation 5]

iv. Detection Limit

Limit of detection (LOD) can be determined by calibration curve in LIBS. It is[] defined as:

$$\mathbf{LOD} = \frac{3 * S_B}{S} \qquad \text{[equation 6]}$$

where,

SB is the standard deviation of background,

S is the slope of calibration.

V. SOFTWARE DEVELOPMENT

We have developed a MATLAB program that defines the peaks as it needed, depends on the threshold that we choose, and we calculate the area under the curve for a 10-shot, and for a one-shot as it necessary, the output of a final is in the form of a table, that contains the location of the point and the area under the curve, the ratio of area in percentage. The program also calculates the SNR for the whole system and SNR, RSD at each wavelength row. The program saved time and its suitable to handle with it . The MATLAB code used Lorentzian fitting .Lorentzian equation is used in our written-MATLAB program, we used it for many reasons such ,it is easy to be calculate , symmetric, and it emphasizes the tails of the peak.

The Lorentzian function is

$$\mathbf{y = y_0 + \frac{2A}{\pi}\frac{w}{4(x-x_C)^2+w^2}} \qquad \text{[equation 7]}$$

Where: y0 = offset, xc = center, w = FWHM, A = area

VI. ORIGIN SOFTWARE

We chose the peak location and the same condition as in MATLAB and calculate the Area under the curve by using Lorentzian fitting manually to compare the results with MATLAB itself.

VII. EXCEL SOFTWARE

We used Excel to calculate the Area und SNR ,LOD for every shot at certain location of the peak.

The Area calculation by using excel was not fitting area under the curve , it was normal calculation of are under curve , so that it is bigger compared to MATLAB and Origin software .

VIII. RESULTS

we chose a threshold that allowed just only peaks with 900 to be appear and calculated we had 44 peaks which some of them are visible in all 10 shots ,as shown in Table 2 , we compared the strong lines with NIST Data base[13].

Table 1. Visible peaks in all 10 shot

Peak location	235.47	242.913	251.569	270.592	279.441	288.032	300.807	303.279	393.36	396.821	589.245
Element	Sn I	Sn I	Si I	Cu II	Mg II	Si I	Fe I	Sn I	Al I	Zn II	S II

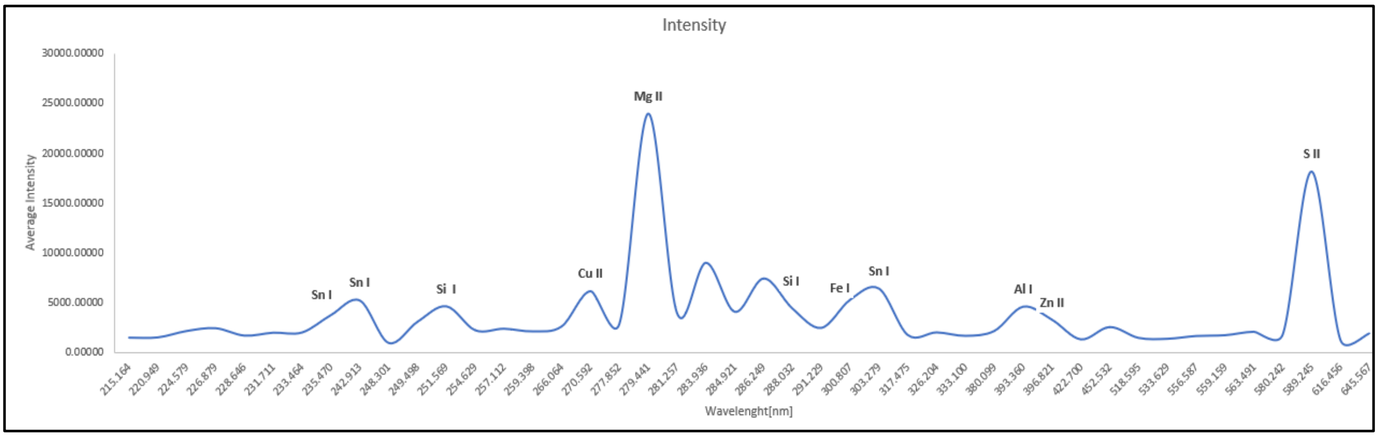

Fig 3. visible peaks at 10 shots

International Journal of Engineering Research and Technology. ISSN 0974-3154, Volume 14, Number 1 (2021), pp. 22-40

IX.I Peak identification

The help of the NIST Database [13], we set the label for the detected peaks as shown in the figure 4

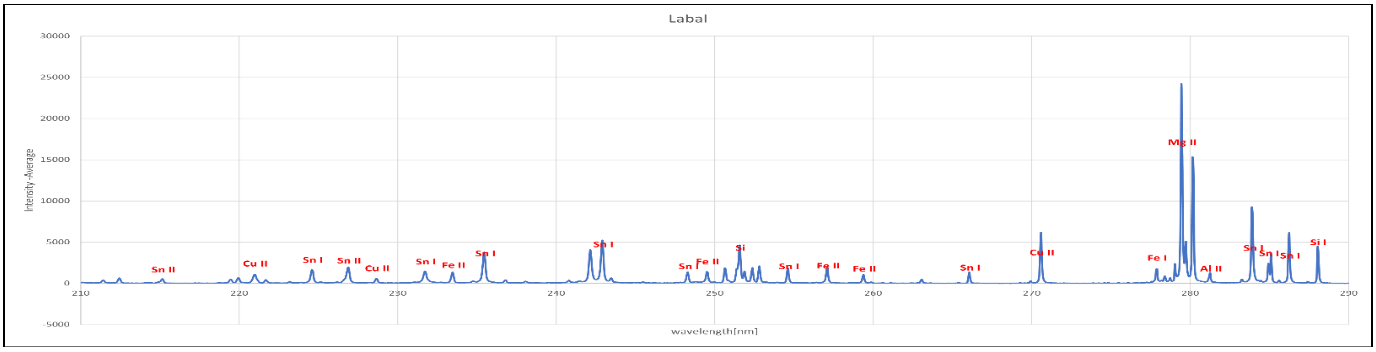

Fig 4 (a)

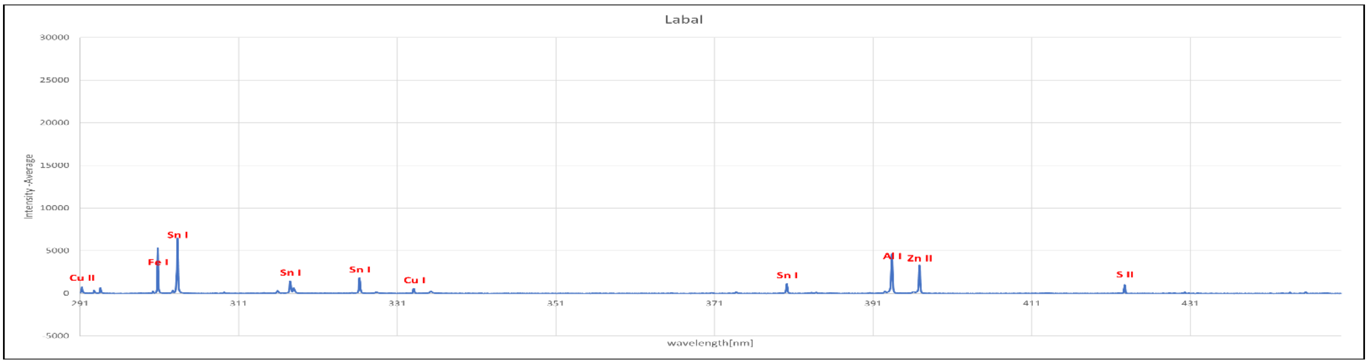

Fig 4(b)

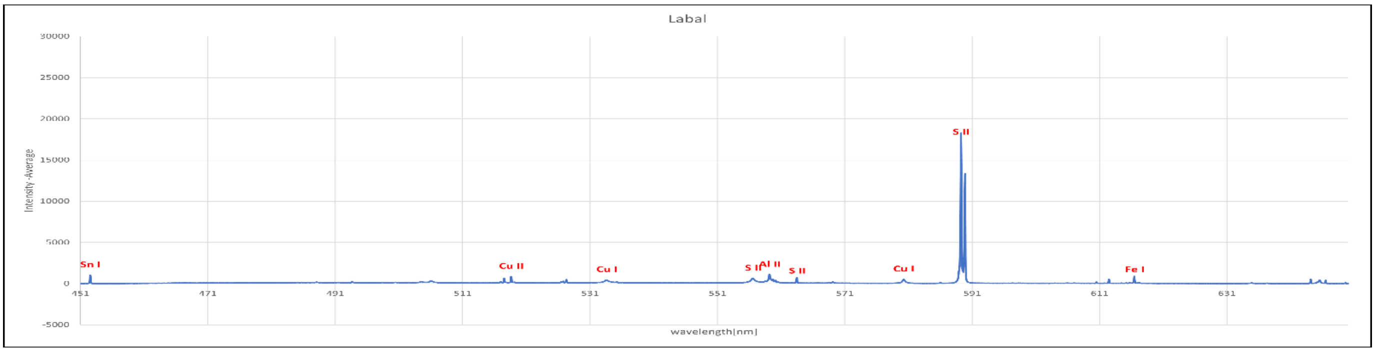

Fig 4 (c)

The intensities 3-D diagram for Origin ,MATLAB, and Excel as shown in Figure 5, Figure 6, and Figure 7,as we see in the figure 4, 5 and figure 6, it is quite visible the effect of the Lorentzian fitting compares with excel 3-d figure with origin and MATLAB 3-D figures.

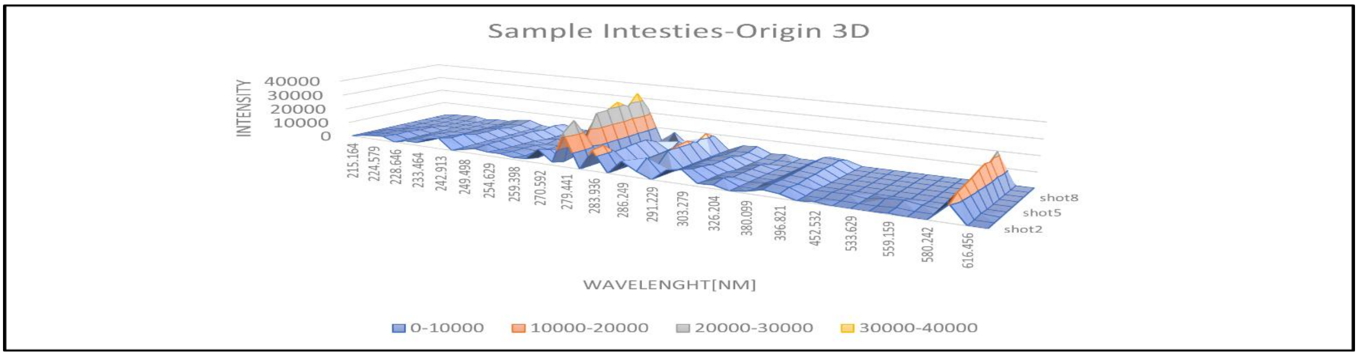

Fig 5. Intensities 3-D Origin

International Journal of Engineering Research and Technology. ISSN 0974-3154, Volume 14, Number 1 (2021), pp. 22-40

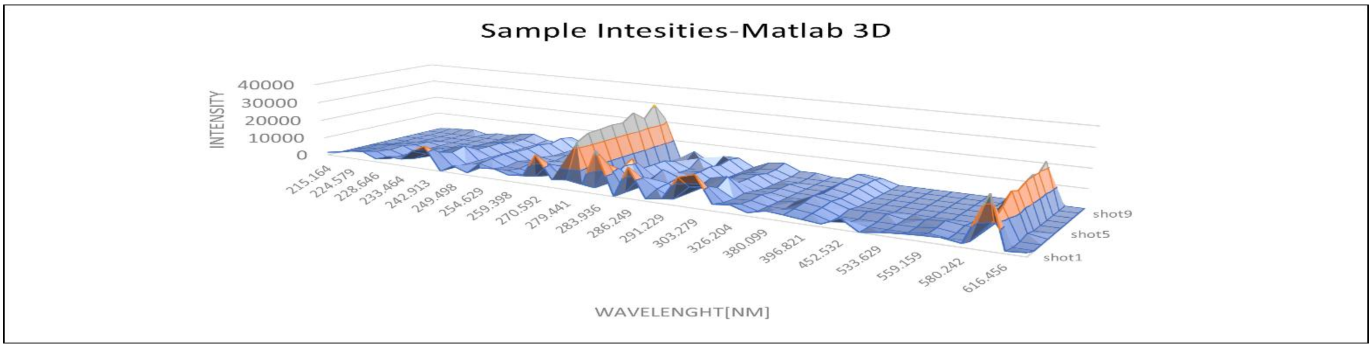

Fig 6. Intensities 3-D MATLAB

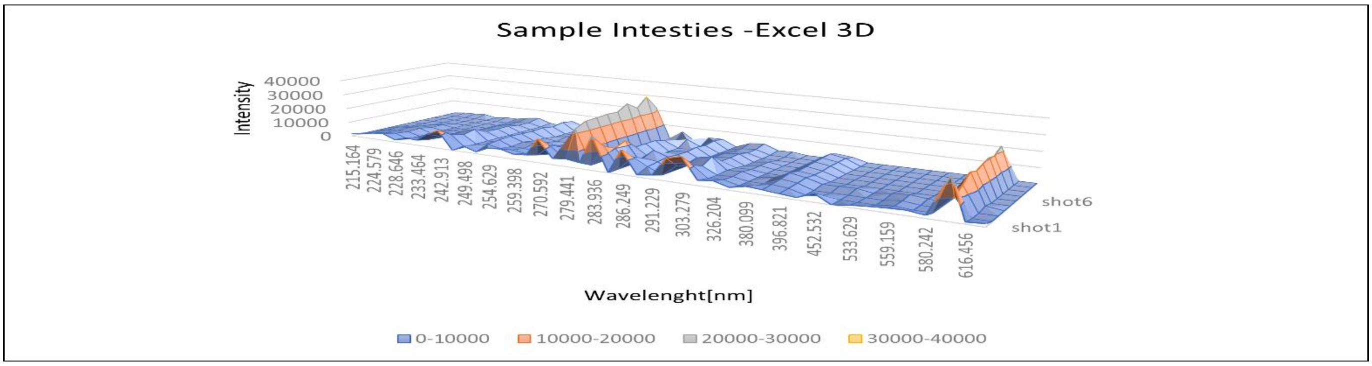

Fig 7. Intensities 3-D Excel

IX.II Limit of Detection

We calculate the limit of detection for every peak at every visible shot, so we have the values of LOD as shown in table[2] , as well the diagram of every shot

Table 2. LOD at each shot

Wavelength[nm]	Shot1	Shot2	Shot3	Shot4	Shot5	Shot6	Shot7	Shot8	Shot9	Shot10
215.164	6.687042									
220.949	3904.518	15033.21	18.63907	2931.1						11633.93
224.579	3.30111	3.705651	5.103684	4.123084	7.097038					11.29238
226.879	2.392877	2.106441	2.60776	2.842951	4.074616	6.364593				4.030971
228.646	6980.792									
231.711	2.6066	2.931313	7.675708	5.18139	7.945669					4.447373
233.464	1.628952	4.131411	5.055947	5.403794						7.747939
235.47	2.181754	2.726351	987.5408	3.234874	4.449603	4.907212	2.094461	5.01664	6.540595	3.724137
242.913	1.790612	2.894816	3.81909	3.118538	3.959998	3.940732	2.252057	3.146831	4.480715	2.08581
248.301										8.466319
249.498	3.385372	5.318794								
251.569	25.85458	25.2607	29.32739	28.41791	24.65338	25.6683	27.09513	25.74008	26.85978	32.77566
254.629	7.253473	1.868336	7.714834	4.671237	7.747826	6.646211				4.70336
257.112	2.508933	3.000612	9.445056	3.263551	6.097653		4.281377			6.381388

International Journal of Engineering Research and Technology. ISSN 0974-3154, Volume 14, Number 1 (2021), pp. 22-40

Wavelength[nm]	Shot1	Shot2	Shot3	Shot4	Shot5	Shot6	Shot7	Shot8	Shot9	Shot10
259.398	3.070458	8.859565		6.459769						
266.064	3.571391	6.637417		6.414822						
270.592	362.0121	83.53708	591.301	2561.311	525.4054	575.5466	3.871764	5.429161	8726.347	2.226398
277.852	3.2125	2.831215		3.901827						
279.441	7.97137	511.6859	0.398331	662.6914	404.3145	64.83237	187.1017	281.785	74.23045	196.5197
281.257	2.155149									
283.936	949.4453	661.1526	1477.157	600.3406	3147.084	1452.187	3453.926	1408.163		2.567489
284.921									9986.006	
286.249	970.9642	327.7922	675.1274	1242.305	3910.762	6.482481				2.338131
288.032	9.795362	379.8661	4.430408	3.762242	3153.874	4.544728	3.37715	809.7769	3.156885	2.144173
291.229	3.908065									
300.807	512.9966	2644.864	1655.136	1846.031	5569.391	4.459684	240.6682	4.401477	7.411046	1.851869
303.279	1131.022	2471.309	46643.6	310.6893	230.2813	751.0947	706.055	5.82628	4749.348	1.179452
317.475	3.382463	3.794345	10.50901	5.856663	4.859925					
326.204	2.805106	3.496181	7.065081	4.599306	6.168263	9.198862	5.017705			
333.1	6.030512									
380.099	2.25784	4.3105		5.068659						
393.36	3.493563	3.549386	4.057019	2.571105	1283.187	3.233065	2.863264	3.966134	2.253872	3.88453
396.821	5.485078	1.617449	4.157734	3.072567	3.602667	3.306767	2.109884	3.367601	1.184948	2.38882
422.7	4.932796			7.292008						
452.532	3.28773	5.894022		7.721021						
518.595				4904.607						
533.629	7.160388									
556.587	6.429071			19.47959						
559.159	4822.075	7.257153	3039.69	11236.69						
563.491	3.674267			6.613367						
580.242	2.692219									
589.245	3817.36	94.36627	146.5534	528.8215	1.348698	351.4796	2.132827	266.4766	519.9721	67.68272
616.456	2099.327			12153.48						
645.567	4.017055									

IX.III Signal Noise Ratio (SNR)

The signal-to-noise ratio (SNR) as shown in figure 8 ,can be considered as tool to explain the signal quality. The SNR compares the average power available in the signal to the average power contained in the noise, which includes any signal from sources other than the target signal source .

In our work we calculate SNR in two different ways :

1. At every peak with the help of Baseline Fluctuation ,where the Standard deviation of it provide us the noise and the peak height provides us the Signal
2. For each Row that included a peak ,that visible for our condition[12]

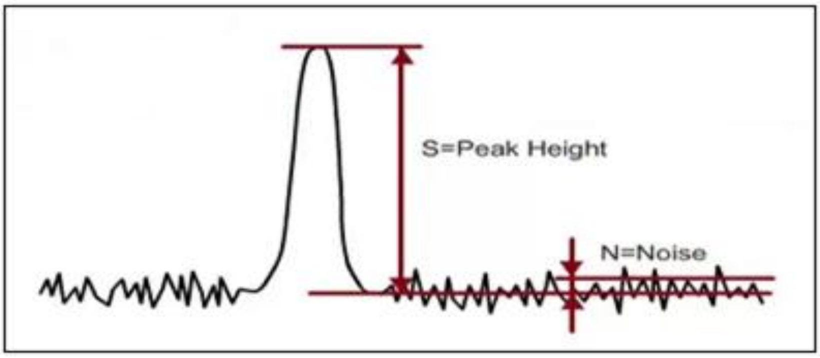

Fig 8. Signal Noise schematic

The LIBS system, that we used , is open to the air conditions , it is obvious that in every single plasma created, there will be other accompanying species in different concentrations in the air just in front of the sample. Furthermore, the laser beam is ablating the sample surface in every shot, so that the shape of the target surface area is changing. Due to this change, laser energy absorbed by the sample is changing shot by shot as well. SNR (Signal to Noise) for every peak at every shot is calculated by equation 5 for every spectrum line observed [12]. The results are shown in Table 3.

Table 3. SNR at each shot

Wavelength[nm]	Shot1	Shot2	Shot3	Shot4	Shot5	Shot6	Shot7	Shot8	Shot9	Shot10
215.164	44.862887									
220.949	0.0768341	0.019956	16.09522	0.102351						0.025787
224.579	90.87853	80.95745	58.781069	72.76106	42.27116					26.56659
226.879	125.37211	142.4203	115.04125	105.5242	73.62656	47.13577				74.42375
228.646	0.0429751									
231.711	115.09245	102.3432	39.08434	57.89953	37.75642					67.45556
233.464	184.16745	72.61441	59.336064	55.51655						38.71997
235.470	137.50402	110.0372	0.3037849	92.73931	67.42174	61.1345	143.2349	59.80098	45.86738	80.55558
242.913	167.54044	103.6335	78.552752	96.19893	75.75762	76.12799	133.2116	95.33401	66.9536	143.829
248.301										35.43453
249.498	88.616546	56.40376								
251.569	11.603358	11.87616	10.229346	10.55672	12.16872	11.68757	11.0721	11.65497	11.16912	9.153133
254.629	41.359498	160.5707	38.886124	64.22282	38.72054	45.1385				63.78419
257.112	119.57276	99.97961	31.762651	91.92442	49.19926		70.07091			47.01172
259.398	97.705299	33.86171		46.44129						
266.064	84.000887	45.19831		46.76669						
270.592	0.8287015	3.59122	0.5073558	0.117128	0.570988	0.521244	77.48407	55.25715	0.034379	134.7468
277.852	93.385214	105.9616		76.88706						

Wavelength[nm]	Shot1	Shot2	Shot3	Shot4	Shot5	Shot6	Shot7	Shot8	Shot9	Shot10
279.441	37.634687	0.586297	753.14334	0.452699	0.741997	4.627318	1.603406	1.064642	4.041468	1.526565
281.257	139.20153									
283.936	0.315974	0.453753	0.2030929	0.499716	0.095326	0.206585	0.086858	0.213044		116.8457
284.921									0.030042	
286.249	0.3089712	0.915214	0.4443606	0.241487	0.076711	46.27858				128.3076
288.032	30.62674	0.789752	67.713847	79.73968	0.095121	66.01055	88.83231	0.370472	95.0304	139.9141
291.229	76.764334									
300.807	0.5847992	0.113427	0.181254	0.162511	0.053866	67.26934	1.246529	68.15894	40.48011	161.9985
303.279	0.2652468	0.121393	0.0064318	0.965595	1.302754	0.399417	0.424896	51.49083	0.063167	254.3554
317.475	88.692757	79.06503	28.546944	51.22371	61.72935					
326.204	106.94784	85.80792	42.462361	65.22723	48.63606	32.61273	59.78829			
333.100	49.747019									
380.099	132.87035	69.59749		59.18725						
393.360	85.872218	84.52167	73.945927	116.6813	0.233793	92.79122	104.7755	75.64041	133.1043	77.22942
396.821	54.693841	185.4773	72.154695	97.63822	83.27164	90.72304	142.1879	89.08419	253.1757	125.585
422.700	60.817432			41.14093						
452.532	91.248382	50.89903		38.85497						
518.595				0.061167						
533.629	41.897169									
556.587	46.663037			15.40074						
559.159	0.0622139	41.33853	0.0986943	0.026698						
563.491	81.648937			45.36267						
580.242	111.43224									
589.245	0.0785883	3.179102	2.0470353	0.567299	222.4367	0.853535	140.6584	1.125803	0.576954	4.432446
616.456	0.142903			0.024684						
645.567	74.681573									

International Journal of Engineering Research and Technology. ISSN 0974-3154, Volume 14, Number 1 (2021), pp. 22-40
© International Research Publication House. http://www.irphouse.com

SNR and RSD% for each Row included the peak with the help of equations [2],[4] are shown in Table 4

Table 4. RSD % and SNR each row

Wavelength [nm]	RSD%	SNR-row
215.164	73.80	1.36
220.949	59.35	1.68
224.579	64.90	1.54
226.879	64.07	1.56
228.646	79.64	1.26
231.711	69.65	1.44
233.464	72.21	1.38
235.470	62.70	1.59
242.913	63.16	1.58
248.301	75.86	1.32
249.498	76.05	1.31
251.569	28.18	3.55
254.629	74.49	1.34
257.112	79.09	1.26
259.398	85.81	1.17
266.064	79.83	1.25
270.592	69.19	1.45
277.852	60.70	1.65
279.441	29.96	3.34
281.257	78.92	1.27
283.936	72.16	1.39
284.921	79.33	1.26
286.249	69.74	1.43
288.032	27.93	3.58
291.229	87.04	1.15
300.807	70.83	1.41
303.279	67.80	1.47
317.475	56.02	1.79
326.204	59.49	1.68
333.100	75.75	1.32
380.099	87.71	1.14
393.360	20.99	4.76
396.821	20.91	4.78
422.700	24.61	4.06
452.532	146.02	0.68
518.595	32.05	3.12
533.629	89.20	1.12
556.587	95.67	1.05
559.159	59.89	1.67
563.491	116.63	0.86
580.242	104.56	0.96
589.245	26.61	3.76
616.456	30.78	3.25
645.567	123.87	0.81

IX.IV RMS(Root Mean Square)

We used RMS to represent the strength of the received signal(data),with help of equation (3) we received the data in table 5 with compare to the peaks at each shot.

Table 5. RMS , Peaks Nr. for each shot

	Peak-Nr	RMS
shot1	41	188.81
shot2	29	112.3637
shot3	23	100.9043
shot4	33	144.4553
shot5	20	73.45588
shot6	16	81.29056
shot7	14	96.43413
shot8	12	80.92402
shot9	12	102.33
shot10	21	51.06672

X. ELEMENTS IN THE SAMPLE:

After determining the peaks, the area under the curve for the total peaks and the ratio of every area to the total Area were calculated, and thus represent the percentage of each element at the sample, or in other words the ratio of each element based on each area under the peak that belong to each element depends on the comparing with NIST database .[13] the compare of the are percentage at each peak between Origin ,MATLAB and Excel show us close results as shown in figure 9, the collected data of the area percentage under curve via Origin ,MATLB and Excel are represented on Tables (6),(7) and (8) .

Table 6. Area percentage from Origin Data

Wavelength[nm]	shot1	shot2	shot3	shot4	shot5	shot6	shot7	shot8	shot9	shot10	Average (row)	Label
215.164	0.546666										0.54666559	Sn II
220.949	1.020265	1.169725	1.028693	0.874376						1.001298	1.01887142	Cu II
224.579	1.575337	1.669832	1.351076	1.209093	0.959616					1.231003	1.33265943	Sn I
226.879	2.175629	2.236934	1.726601	1.617817	1.199775	1.198761				1.756711	1.7017467	Sn II
228.646	0.656454										0.65645382	Cu II
231.711	1.900948	1.710156	1.274023	1.335433	1.055023					1.387527	1.44385153	Sn I
233.464	1.33237	1.313004	1.01193	0.992216						0.97458	1.12481976	Fe II
235.47	3.882835	3.970772	3.057082	2.872599	2.240596	2.172033	2.098576	1.612731	1.331305	3.005184	2.62437141	Sn I
242.913	6.67512	5.602859	4.335957	4.235727	3.051859	3.057992	2.94252	2.267565	1.859483	4.139767	3.81688493	Sn I
248.301										0.904395	0.9043954	Sn I
249.498	1.52026	1.418707									1.46948327	Fe II
251.569	0.505025	3.240012	4.403412	3.480777	4.922068	4.899526	5.213806	5.134668	5.627344	5.626995	4.30536334	Si I
254.629	1.615405	1.436472	1.034575	1.174574	0.817623	0.769939				1.258688	1.15818246	Sn I
257.112	1.946506	1.656617	1.111021	1.365766	0.881706		0.821178			1.217824	1.28580254	Fe II
259.398	1.093342	0.872455		0.73547							0.90042234	Fe II
266.064	1.131758	0.941031		0.771346							0.94804532	Sn I
270.592	5.289031	5.03915	3.548167	3.749535	2.697897	2.553074	2.45657	1.951644	1.628223	3.453375	3.23666652	Cu II
277.852	1.375721	1.359608		1.308602							1.34797718	Fe I
279.441	1.53183	17.40053	24.67449	18.26212	28.14388	28.73219	31.1638	29.45407	33.12065	28.76946	24.1253026	Mg II
281.257	1.245226										1.24522626	Al II
283.936	8.906691	8.341102	6.313101	6.317653	4.554032	4.700154	4.354078	3.465528		5.679704	5.84800494	Sn I
284.921									2.624834		2.62483354	Sn I
286.249	5.239265	4.800099	3.317236	3.753784	2.556416	2.584659				3.495987	3.67820681	Sn I
288.032	0.39081	1.982284	2.748164	2.388033	2.952199	2.926295	3.252687	3.281253	3.457871	3.469555	2.68491494	Si I
291.229	0.871165										0.87116452	Cu II
300.807	4.546481	3.948475	2.630894	3.238951	2.291402	2.136281	2.073953	1.677193	1.340337	2.88381	2.67677775	Fe I
303.279	6.91988	5.824688	3.980094	4.982148	3.36339	3.303607	3.266772	2.463992	2.076254	4.382861	4.05636854	Sn I
317.475	1.089824	1.088547	0.950414	1.035521	0.946982					1.076934	1.03137043	Sn I
326.204	1.410144	1.250658	0.975471	1.058447	0.841817	0.917776	0.865751			0.914081	1.02926811	Sn I
333.1	0.468623										0.46862315	Cu I

Wavelength[nm]	shot1	shot2	shot3	shot4	shot5	shot6	shot7	shot8	shot9	shot10	Average (row)	Label
380.099	1.069532	0.693219		0.62158							0.79477703	Sn I
393.36	0.869916	2.08727	3.059436	2.775099	3.159935	3.704543	4.00261	5.046416	4.521127	3.419309	3.26456617	Al I
396.821	0.555607	1.888723	2.171399	1.931658	2.197615	2.422854	2.832323	3.448302	3.065102	2.457351	2.29709338	Zn II
422.7	0.365187			0.571041							0.46811365	S II
452.532	2.005262	0.622049		0.76308							1.13013012	Sn I
518.595				0.734137							0.73413694	Cu II
533.629	1.039105										1.03910473	Cu I
556.587	1.779391			0.616739							1.1980649	S II
559.159	2.016792	0.990317	1.305747	0.916117							1.30724307	Al II
563.491	1.076491			0.55105							0.81377042	S II
580.242	1.233028										1.23302767	Cu I
589.245	20.4196	15.44471	23.99102	23.19728	31.16616	33.92032	34.65537	40.19664	40.23665	17.4936	28.0721347	S II
616.456	0.39072			0.562229							0.47647446	Fe I
645.567	0.969008										0.96900838	Sn II

Table 7. Area percentage from MATLAB Data

Wavelength [nm]	shot1	shot2	shot3	shot4	shot5	shot6	shot7	shot8	shot9	shot10	Average (row)	Label
215.164	0.4080231										0.408023145	Sn II
220.949	0.8181241	0.861566	0.667377	0.5736311						0.66285	0.716709648	Cu II
224.579	1.3212006	1.361857	1.017679	0.9338715	0.6828317					0.9603261	1.046294351	Sn I
226.879	1.8836007	1.832722	1.258865	1.2030437	0.8011692	0.801069				1.4777144	1.322597717	Sn II
228.646	0.4912569										0.491256916	Cu II
231.711	1.4827446	1.228672	0.810553	0.8867392	0.6676306					1.0575949	1.022322304	Sn I
233.464	1.163993	1.08208	0.759491	0.7909703						0.8079399	0.920894763	Fe II
235.47	3.6145259	3.493675	2.472163	2.419709	1.7211121	1.5973555	1.5103283	1.107186	0.8842452	2.5973048	2.141760481	Sn I
242.913	7.5666243	5.09828	3.575512	3.7392464	2.3023336	2.2472974	2.2576359	1.6590532	1.2145647	3.7114579	3.337200526	Sn I
248.301										0.763186	0.763186011	Sn I
249.498	1.2824294	1.121998									1.202213569	Fe II
251.569	0.3367143	2.643308	3.393413	2.776544	3.8008814	3.6487297	3.8287671	3.7213194	3.8924339	4.7240201	3.276613082	Si I
254.629	1.6121273	1.327171	0.848468	1.0917939	0.6659174	0.6232556				1.1860474	1.050683059	Sn I
257.112	1.8790837	1.488395	0.837623	1.2224106	0.7249149		0.6493755			1.1314412	1.133320533	Fe II
259.398	1.0126424	0.68492		0.6191965							0.772253125	Fe II
266.064	1.1765955	0.899876		0.782718							0.95306317	Sn I
270.592	5.8091992	5.361764	3.56458	3.870448	2.6016818	2.367944	2.2576062	1.7246749	1.3869184	3.6139567	3.25587728	Cu II
277.852	1.2758948	1.046059		0.9969652							1.106306314	Fe I
279.441	1.5101041	13.34201	18.74037	13.59947	22.200697	23.180216	25.75382	25.779426	27.902029	22.160121	19.41682609	Mg II

International Journal of Engineering Research and Technology. ISSN 0974-3154, Volume 14, Number 1 (2021), pp. 22-40

Wavelength [nm]	shot1	shot2	shot3	shot4	shot5	shot6	shot7	shot8	shot9	shot10	Average (row)	Label
281.257	1.1904477										1.19044769	Al II
283.936	9.5553212	8.386237	6.086626	6.0875048	4.0516362	4.1537619	3.8311434	3.1881905		5.8379873	5.686489734	Sn I
284.921									2.2165083		2.216508278	Sn I
286.249	5.7647818	5.173756	3.25274	3.8428706	2.3658166	2.3485908				3.6921249	3.777240134	Sn I
288.032	0.3471487	1.96509	2.64658	2.3666434	2.8238101	2.7426689	2.9929137	3.0550885	3.0506652	3.7756841	2.576629283	Si I
291.229	0.7071106										0.70711063	Cu II
300.807	4.8898334	4.219003	2.613038	3.3272566	2.1857404	2.0434034	1.9507405	1.5356995	1.164387	3.2008083	2.712991012	Fe I
303.279	6.5618867	5.524976	3.547032	4.4846722	2.734504	2.7258026	2.6927609	1.9358402	1.6192107	4.2927935	3.611947873	Sn I
317.475	1.0685783	0.920448	0.693153	0.7880037	0.6205635					0.7824725	0.812203088	Sn I
326.204	1.3988333	1.190144	0.973319	0.974381	0.7485575	0.7764232	0.7313866			0.9294678	0.965314034	Sn I
333.1	0.4673317										0.467331724	Cu I
380.099	1.1259144	0.678981		0.5212758							0.77539024	Sn I
393.36	0.9144723	1.962311	2.832562	2.5947838	2.8344632	3.3369106	3.5103467	4.6458647	3.8840759	3.2357098	2.97515001	Al I
396.821	0.6033394	1.419213	1.93588	1.7537981	1.9063903	2.012094	2.4394504	3.123593	2.5726481	2.3484398	2.011484605	Zn II
422.7	0.3761329			0.4854669							0.43079992	S II
452.532	1.622667	0.509038		0.5251617							0.885622194	Sn I
518.595				0.5560191							0.556019125	Cu II
533.629	0.4942984										0.494298381	Cu I
556.587	1.0823853			0.5872526							0.834818978	S II
559.159	1.3889861	0.518275	0.609813	0.9451113							0.865546379	Al II
563.491	0.9270146			0.3847467							0.655880648	S II
580.242	0.6755818										0.675581774	Cu I
589.245	23.21903	16.54114	24.99492	24.451972	31.672973	34.290535	34.77376	41.174773	39.775063	13.831875	28.4726045	S II
616.456	0.2970398			0.4910242							0.394031972	Fe I
645.567	0.6335282										0.633528243	Sn II

Table 8. Area percentage from Excel Data

Wavelength [nm]	shot1	shot2	shot3	shot4	shot5	shot6	shot7	shot8	shot9	shot10	Average (row)	Label
215.164	0.685308										0.685308026	Sn II
220.949	1.222406	1.477884	1.390008	1.175122						1.339745	1.32103319	Cu II
224.579	1.829474	1.977806	1.684473	1.484314	1.236401					1.501679	1.619024512	Sn I
226.879	2.467658	2.641146	2.194336	2.03259	1.598381	1.596452				2.035707	2.080895686	Sn II
228.646	0.821651										0.821650714	Cu II
231.711	2.319151	2.19164	1.737493	1.784126	1.442414					1.717459	1.865380747	Sn I
233.464	1.500746	1.543927	1.264369	1.193462						1.141219	1.32874475	Fe II
235.47	4.151144	4.447869	3.642	3.325489	2.76008	2.746711	2.686824	2.118277	1.778366	3.413063	3.106982337	Sn I
242.913	5.783616	6.107438	5.096403	4.732208	3.801385	3.868686	3.627404	2.876076	2.504401	4.568076	4.296569341	Sn I

International Journal of Engineering Research and Technology. ISSN 0974-3154, Volume 14, Number 1 (2021), pp. 22-40

Wavelength [nm]	shot1	shot2	shot3	shot4	shot5	shot6	shot7	shot8	shot9	shot10	Average (row)	Label
248.301										1.045605	1.045604791	Sn I
249.498	1.75809	1.715416									1.736752971	Fe II
251.569	0.673335	3.836716	5.413411	4.18501	6.043255	6.150322	6.598845	6.548017	7.362255	6.52997	5.334113597	Si
254.629	1.618682	1.545773	1.220682	1.257354	0.969329	0.916623				1.331329	1.265681864	Sn I
257.112	2.013927	1.824838	1.384419	1.509121	1.038497		0.992981			1.304208	1.438284555	Fe II
259.398	1.174041	1.05999		0.851743							1.02859156	Fe II
266.064	1.086921	0.982186		0.759975							0.943027477	Sn I
270.592	4.768863	4.716536	3.531754	3.628622	2.794111	2.738204	2.655533	2.178613	1.869528	3.292793	3.217455758	Cu II
277.852	1.475548	1.673157		1.620239							1.589648052	Fe I
279.441	1.553557	21.45904	30.60861	22.92477	34.08707	34.28416	36.57379	33.12872	38.33928	35.3788	28.83377903	Mg II
281.257	1.300005										1.300004835	Al II
283.936	8.258061	8.295968	6.539577	6.547802	5.056428	5.246545	4.877013	3.742866		5.521422	6.00952015	Sn I
284.921									3.033159		3.033158794	Sn I
286.249	4.713749	4.426442	3.381732	3.664698	2.747016	2.820728				3.29985	3.579173478	Sn I
288.032	0.434471	1.999478	2.849747	2.409422	3.080588	3.10992	3.512461	3.507417	3.865077	3.163425	2.793200603	Si I
291.229	1.035218										1.035218407	Cu II
300.807	4.203129	3.677946	2.64875	3.150645	2.397064	2.229159	2.197166	1.818687	1.516288	2.566812	2.640564494	Fe I
303.279	7.277873	6.124399	4.413157	5.479624	3.992277	3.881412	3.840783	2.992144	2.533297	4.472928	4.500789212	Sn I
317.475	1.111069	1.256647	1.207675	1.283039	1.273401					1.371395	1.250537768	Sn I
326.204	1.421455	1.311173	0.977623	1.142513	0.935076	1.059129	1.000115			0.898693	1.093222189	Sn I
333.1	0.469915										0.469914575	Cu I
380.099	1.013151	0.707457		0.721884							0.814163828	Sn I
393.36	0.82536	2.21223	3.286309	2.955414	3.485407	4.072176	4.494874	5.446967	5.158178	3.602909	3.553982328	Al I
396.821	0.507874	2.358232	2.406919	2.109518	2.488839	2.833613	3.225196	3.773012	3.557556	2.566263	2.582702158	Zn II
422.7	0.354241			0.656614							0.505427379	S II
452.532	2.387857	0.735059		1.000998							1.374638037	Sn I
518.595				0.912255							0.912254751	Cu II
533.629	1.583911										1.583911087	Cu I
556.587	2.476397			0.646225							1.561310818	S II
559.159	2.644597	1.462359	2.001681	0.887123							1.748939756	Al II
563.491	1.225968			0.717353							0.971660194	S II
580.242	1.790474										1.790473566	Cu I
589.245	17.62016	14.34828	22.98711	21.9426	30.65935	33.5501	34.53698	39.2185	40.69823	21.15533	27.67166486	S II
616.456	0.484401			0.633433							0.558916952	Fe I
645.567	1.304489										1.304488507	Sn II

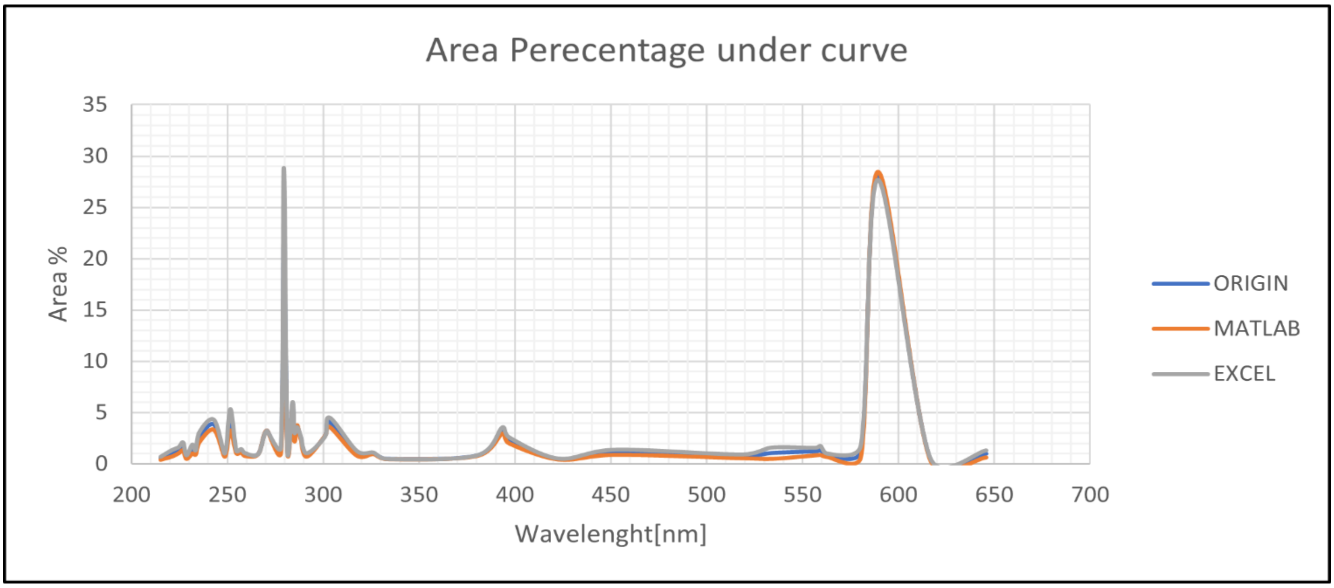

Fig 9. Area percentage under curve

Elements percentage via Origin software are shown in Table 9

Table 9. Element percentage via Origin software

Element %	shot1	shot2	shot3	shot4	shot5	shot6	shot7	shot8	shot9	shot10
Aluminum %	4.131933734	3.077587	4.365183	3.691216	3.159935	3.704543	4.00261	5.046416	4.521127	3.419309
Cupper %	10.5776703	6.208875	4.57686	5.358048	2.697897	2.553074	2.45657	1.951644	1.628223	4.454672
Iron %	12.2053995	10.56887	4.753844	8.203234	3.173108	2.136281	2.895132	1.677193	1.340337	5.076214
Magnesium %	1.531830301	17.40053	24.67449	18.26212	28.14388	28.73219	31.1638	29.45407	33.12065	28.76946
Sulfur %	23.6406645	15.44471	23.99102	24.93611	31.16616	33.92032	34.65537	40.19664	40.23665	17.4936
Silicon %	0.895834218	5.222296	7.151576	5.86881	7.874267	7.82582	8.466494	8.415921	9.085216	9.09655
Tin %	47.11330514	40.18842	28.31563	31.7488	21.58713	18.70492	13.5277	9.809817	7.891875	29.23284
Zink %	0.555606556	1.888723	2.171399	1.931658	2.197615	2.422854	2.832323	3.448302	3.065102	2.457351

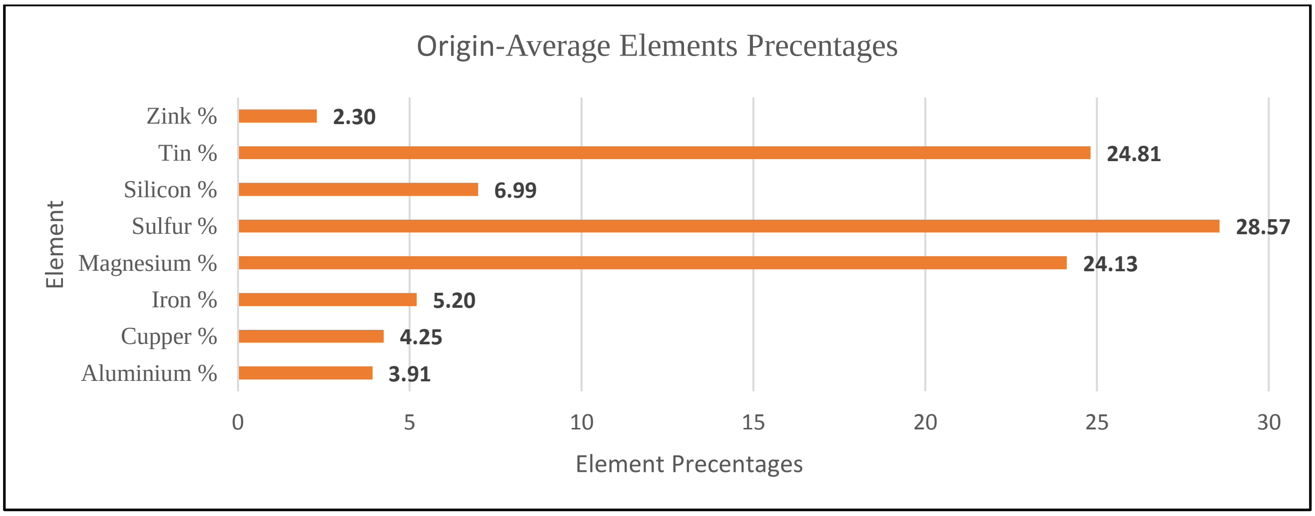

Chart 1. Average elements percentage by using Origin-software

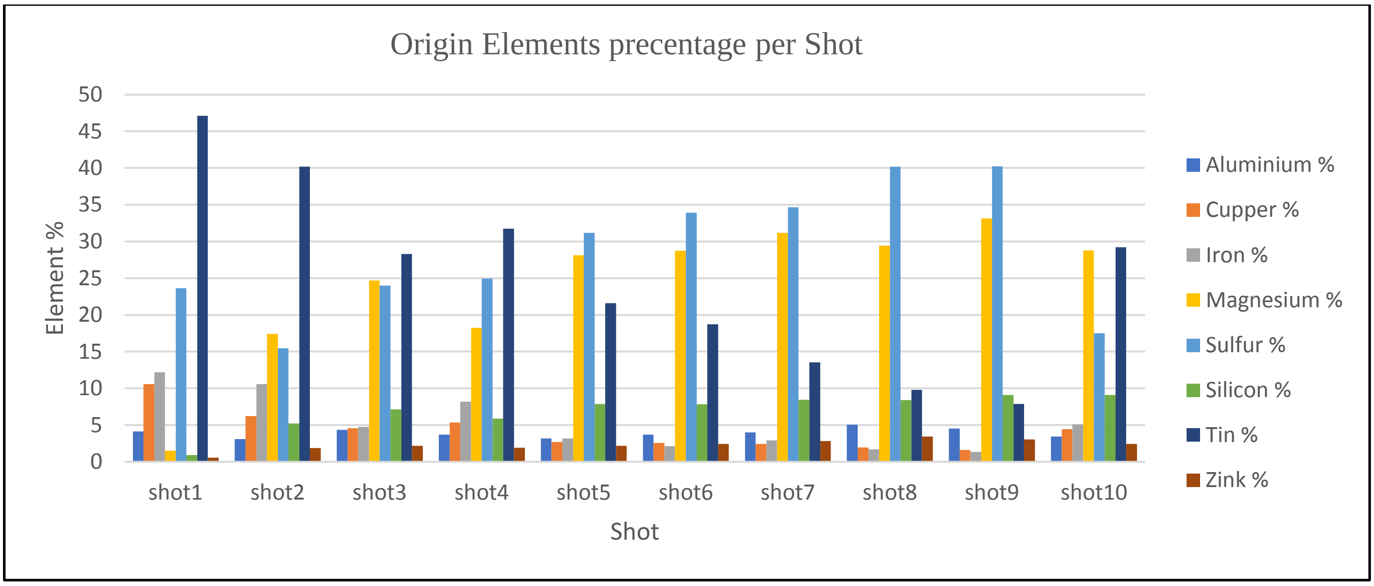

Chart 2. Elements percentage per Shot by using Origin-software

Elements percentage via MATLAB software are shown in Table 10

Table 10. Element percentage via Origin software

	shot1	shot2	shot3	shot4	shot5	shot6	shot7	shot8	shot9	shot10
Aluminum %	3.493906	2.480585	3.442376	3.539895	2.834463	3.336911	3.510347	4.645865	3.884076	3.23571
Cupper %	9.462903	6.22333	4.231957	5.000098	2.601682	2.367944	2.257606	1.724675	1.386918	4.276807
Iron %	11.80092	9.642456	4.210151	7.447823	2.910655	2.043403	2.600116	1.5357	1.164387	5.140189
Magnesium %	1.510104	13.34201	18.74037	13.59947	22.2007	23.18022	25.75382	25.77943	27.90203	22.16012
Sulfur %	25.60456	16.54114	24.99492	25.90944	31.67297	34.29054	34.77376	41.17477	39.77506	13.83188
Silicon %	0.683863	4.608398	6.039994	5.143187	6.624691	6.391399	6.821681	6.776408	6.943099	8.499704
Tin %	46.79695	37.62583	24.53611	28.28099	17.36207	15.27356	11.02326	7.89027	5.934529	27.28848
Zink %	0.603339	1.419213	1.93588	1.753798	1.90639	2.012094	2.43945	3.123593	2.572648	2.34844

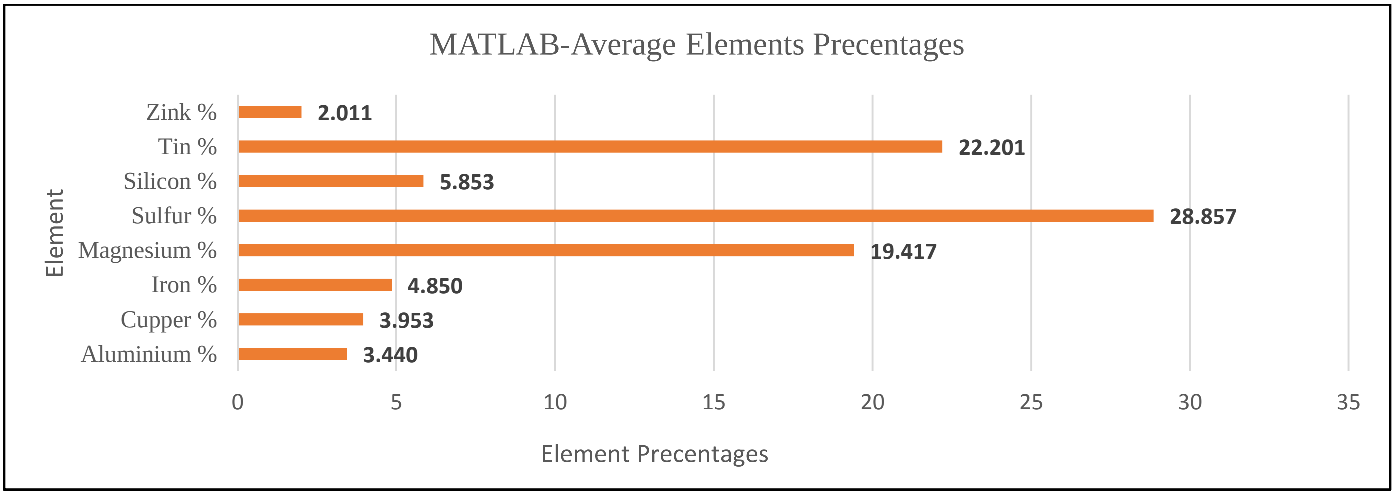

Chart 3. Average elements percentage by using MATLAB-software

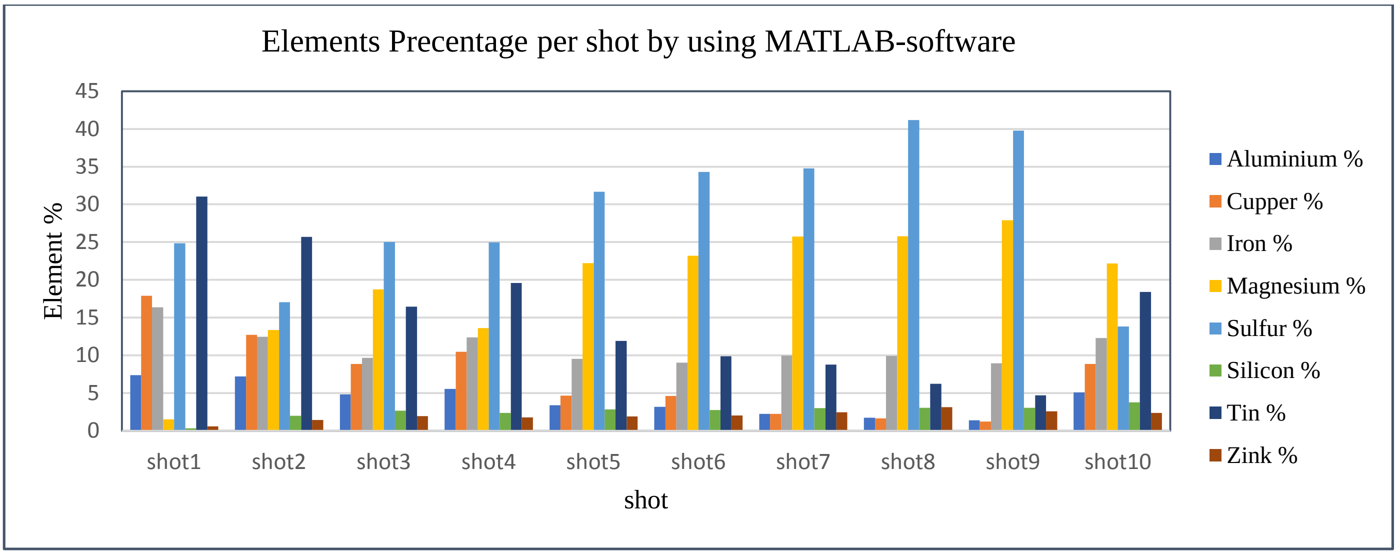

Chart 4. Elements percentage per Shot by using MATLAB-software

Table 11. Element percentage via Excel software

	shot1	shot2	shot3	shot4	shot5	shot6	shot7	shot8	shot9	shot10
Aluminum %	4.76996	3.67459	5.28799	3.84254	3.48541	4.07218	4.49487	5.44697	5.15818	3.60291
Cupper %	11.69244	6.19442	4.92176	5.71600	2.79411	2.73820	2.65553	2.17861	1.86953	4.63254
Iron %	12.60988	11.49528	5.29754	8.95864	3.43556	2.22916	3.19015	1.81869	1.51629	5.01224
Magnesium %	1.55356	21.45904	30.60861	22.92477	34.08707	34.28416	36.57379	33.12872	38.33928	35.37880
Sulfur %	21.67677	14.34828	22.98711	23.96279	30.65935	33.55010	34.53698	39.21850	40.69823	21.15533
Silicon %	1.10781	5.83619	8.26316	6.59443	9.12384	9.26024	10.11131	10.05543	11.22733	9.69340
Tin %	47.42966	42.75101	32.09515	35.21661	25.81219	22.13629	16.03214	11.72936	9.84922	31.17720
Zink %	0.50787	2.35823	2.40692	2.10952	2.48884	2.83361	3.22520	3.77301	3.55756	2.56626

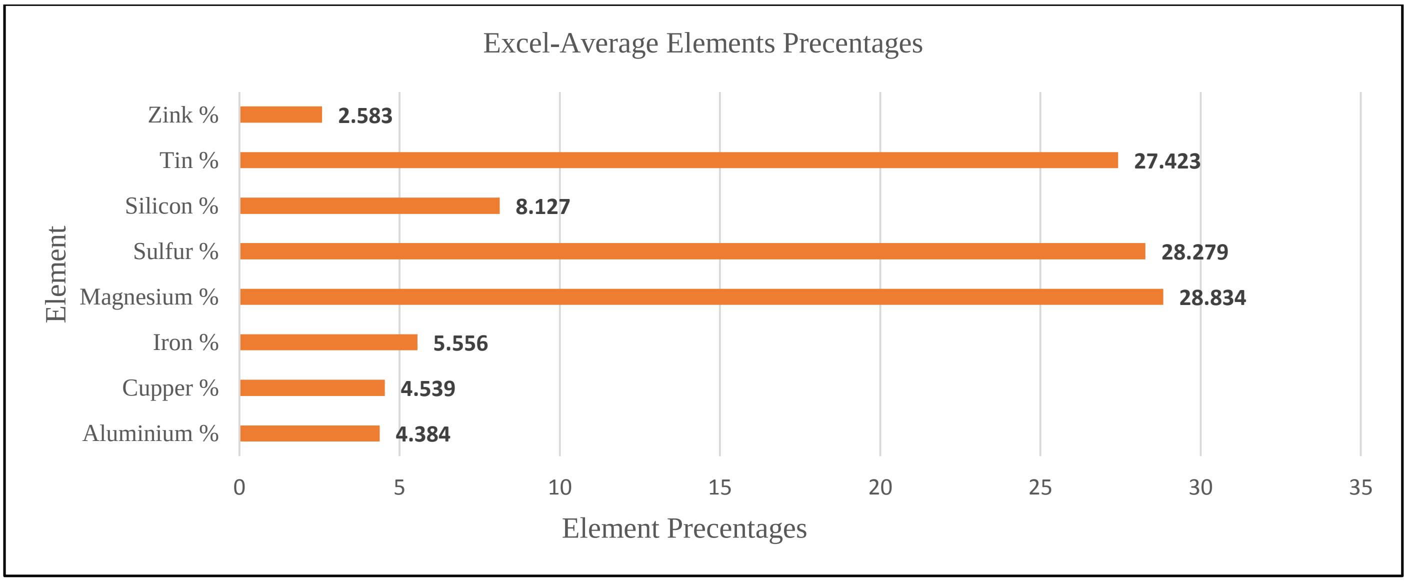

Chart 5. Average elements percentage by using Excel-software

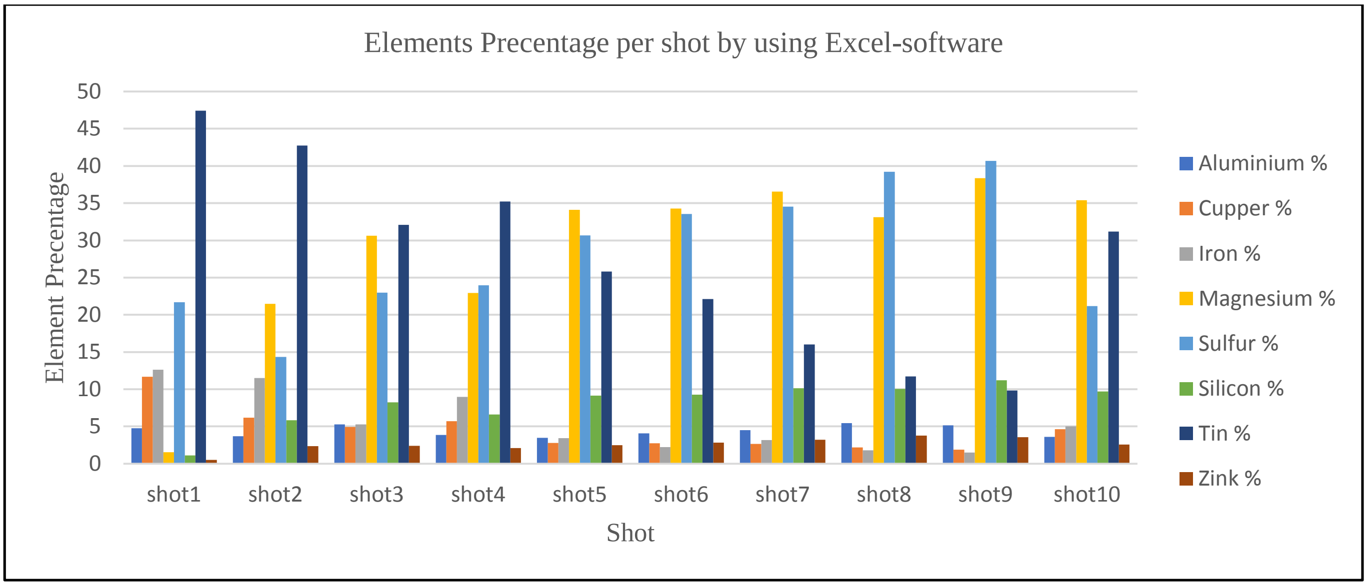

Chart 6. Elements percentage per Shot by using Excel-software

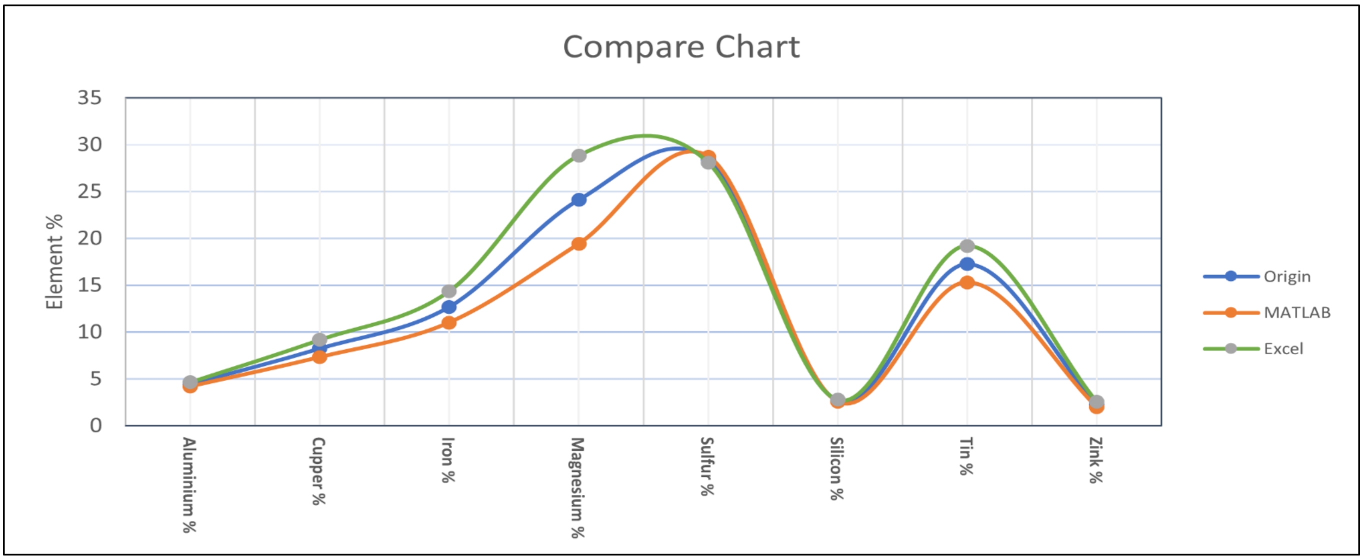

Figure 16. Compare the Average Area percentage between MATLAB, Origin and Excel

XI. CONCLUSION

The results that are shown of the investigated elements, the MATLAB code was running smoothly and rapid, the area percentage on MATLAB was smaller than in origin and excel. This was affected of the Lorentzian fitting and changing of FHWM. The condition of the investigation experiment could be effecting the results. Other strong line data bases for the elements can be added to the code so that the software can determine the wavelength for each element by comparing .

REFERENCE

[1] J Hecht,"Short history of laser development ", Opt. Eng. 49(9), 091002 (September 01, 2010).

[2] W. Demtroder, "Laser Spectroscopy Basic Concepts and Instrumentation", Springer, 1996.

[3] L.Radziemski, Solarz R.W., Paisner J. A., "Laser Spectroscopy and Its Applications", Marcel Dekker Inc., 1987.

[4] A. J. Miziolek, V. Palleschi, I. Schechter, "Laser- Induced Breakdown Spectroscopy", Cambridge, 2006.

[5] Cremers, D.A., Radziemski, L.J. Handbook of Laser-Induced Breakdown Spectroscopy, Chichester, UK: John Wiley and Sons, 2006.

[6] Paul Dirac,"The Quantum Theory of Emission and Absorption of Radiation". In: Proc. Roy. Soc. A114, 1927

[7] S. Cosentino, et al., The Role of The Surfaces in The Photon Absorption In Ge Nanoclusters Embedded In Silica, Nanoscale Research Letters, 6, 135 – 141, 2011

International Journal of Engineering Research and Technology. ISSN 0974-3154, Volume 14, Number 1 (2021), pp. 22-40

[8] R. Wisburn, I. Schechter, R. Niesser, H. Schroder and K. I. Kompa, “Analytic Chemistry”, 66, 2964, 1994

[9] DAVID A. CREMERS J. RADZIEMSKI, “Handbook of Laser-Induced Breakdown Spectroscopy Second Edition”, chapter3,2013

[10] Daeyeon Lee, Michael F. Rubner and Robert E. Cohen Nano, “All-Nanoparticle Thin-Film Coatings” LettersVol. 6: , Issue. 10, : Pages. 2305-2312,, 2006

[11] L.Caneve, F.Colao , F.Sarto, V.Spizzichino , M.Vadrucci, “Laser-induced breakdown spectroscopy as a diagnostic tool for thin films elemental composition Spectrochimica Acta” Part B: Atomic Spectroscopy Volume 60, Issues 7–8, 31, Pages 1098-1102, 2005

[12] Elisabetta Tognoni , Gabriele Cristoforetti,“ Review Signal and noise in Laser Induced Breakdown Spectroscopy: An introductory review,2015

[13] Atomic Spectra Database | NIST